PROCEEDINGS, 50th Workshop on Geothermal Reservoir Engineering
Stanford University, Stanford, California, February 10-12, 2025
SGP-TR-229

EGS Reservoir Characterization Through Injectivity and Steady-State Circulation Tests

Deniz Ertaş

ExxonMobil Technology and Engineering Company, 1545 Rte 22 East, Annandale, NJ 08801

deniz.ertas@exxonmobil.com

Keywords: injectivity, leakoff, circulation, reservoir model

ABSTRACT

Accurate and robust characterization of the stimulated rock volume around EGS wells is critical to understanding and optimizing reservoir performance. Commercially successful stimulations need to produce a highly connected set of wells to minimize hydraulic losses at commercial rates of circulation, create uniform fracture permeability to avoid thermal short-circuiting, and the created fracture permeability needs to exceed the background (matrix) permeability of the surrounding rock to minimize leak-off. A simple set of post-stimulation well tests are proposed to obtain key reservoir parameters that can be used to quickly build a simple hydraulic circuit model that can be solved analytically. This model can then be used to evaluate important reservoir characteristics. The analysis does not consider thermomechanical and buoyancy effects but provides a good starting point for building more sophisticated reservoir models as more production data becomes available.

This approach was applied to the circulation test data for Fervo's Project Red pilot published in Norbeck and Latimer (2023) to inform fracture and matrix permeabilities, deduce the shape and evolution of the thermal front, and estimate best-case reservoir performance. The transient injectivity and steady-state circulation flow analysis yielded an average stimulated reservoir volume (SRV) permeability of 2.5 – 2.8 md surrounding the injector-producer pair, and a matrix permeability of about 0.3 md in the far field. A simple reservoir model with uniform SRV permeability was built around this data and was subsequently used to analytically estimate long-term performance in steady-state production at a rate of 40 l/s that was demonstrated during the circulation test. The projected thermal breakthrough time is about 5 years, with the flow forming a relatively sharp thermal front between the injector and producer, i.e., with a width that is about one quarter of the front propagation distance.

Under these simplifying assumptions, temperature drop of the produced fluid is expected to be minimal during most of the project cycle. A relatively steep temperature drop is expected after about 4 years, when the broadened thermal front approaches the producer.

1. INTRODUCTION

The adaptation of state-of-the-art unconventional oil&gas drilling and completions practices has revolutionized development of enhanced geothermal systems in recent years. Notably, Fervo Energy has conducted a proof-of-principle pilot study in Blue Mountain, Nevada ("Project Red") to demonstrate the efficacy of drilling and stimulating a horizontal injector-producer pair (Norbeck and Latimer 2023) and is applying the learnings to their commercial project in Milford, Utah (Norbeck et al. 2024).

The ability to cost-effectively drill and stimulate injector and producer wells is necessary for commercial success. However, it is equally important to minimize hydraulic energy losses while creating a uniform thermal front with high thermal sweep efficiency and avoiding thermal short-circuiting and leak-off. In a successful application, multi-stage, multi-cluster stimulations are performed to produce uniformly spaced fracture clusters that connect injector wells to producer wells. Proper planning, execution and analysis of injection, production and circulation tests are critical in the early evaluation of the stimulated rock volume (SRV) and its surrounding rock matrix.

One of the goals of this manuscript is to convey the importance of well tests and the sharing of data from such tests to build confidence in the performance projections of the given wellfield. Of utmost importance is a quantitative understanding of the hydraulic resistance between injector-producer pairs, which impacts expected parasitic losses as well as the propagation of the thermal front from injector towards producer. As an example, circulation test results presented in Norbeck and Latimer (2023) was utilized to build a simple hydraulic model for the injector-producer pair that is consistent with available data and to infer basic characteristics of the reservoir and its future performance.Monitoring of the interwell pressure drop during production as well as the evolution of the production temperature will allow the operator to identify and potentially mitigate thermal short-circuiting phenomena.

The manuscript is organized as follows: In Section 2, circulation test data from Project Red is analyzed to infer a simple reservoir model that is consistent with both transient and quasi-steady state flow. The utility of this model is demonstrated by predicting the thermal breakthrough time of this well pair. In Section 3, an attempt has been made to design a reservoir for a commercial project, where the lateral length and well spacing has been increased to optimize circulation rates and thermal breakthrough time. The learnings are consistent with practices that have been adopted by Fervo in their Cape Station project. Section 4 discusses the limitations of the simple model and proposes gradual relaxation of assumptions and numerical approaches to identify deviations to diagnose potential problems.

2. ANALYSIS OF PROJECT RED CIRCULATION DATA

Information about the Project Red wells, and circulation test was obtained from Norbeck and Latimer (2023) and digitized for the following hydraulics analysis. This is an EGS doublet configuration where the horizontal injector and producer are at 7500ft total vertical depth (TVD) and have subparallel horizontal sections that are L=365 ft apart on average. The wells were stimulated along 2400 ft of lateral sections with 16 stages, 6 clusters/stage, and a stage length of 150 ft. The data is reproduced in Figure 1.

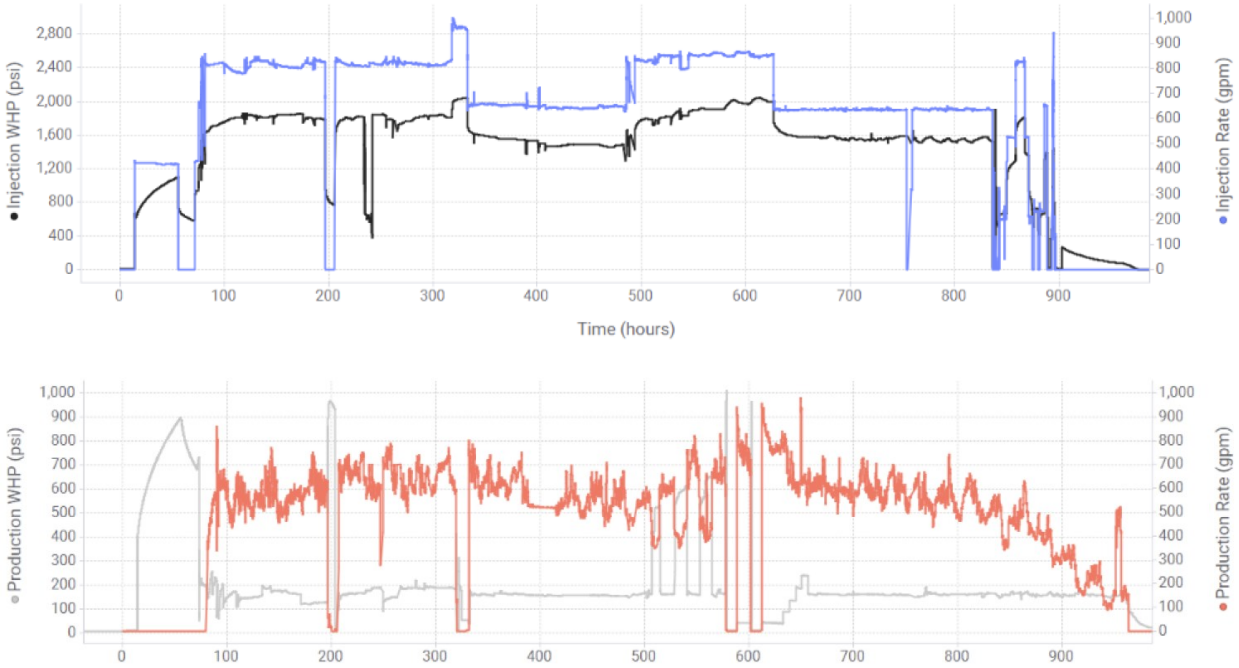

Figure 1: Fervo pilot injector and producer history, reproduced from Norbeck and Latimer (2023)

2.1 Inference of reservoir properties

The data has many transients that are hard to interpret, but there are two specific time intervals that were amenable to quantitative analysis. The analysis was based on a reservoir model with a uniform fracture permeability within the SRV which extends well beyond the injector-producer pair, and a uniform matrix permeability in the surrounding unfractured rock, see Figure 2.

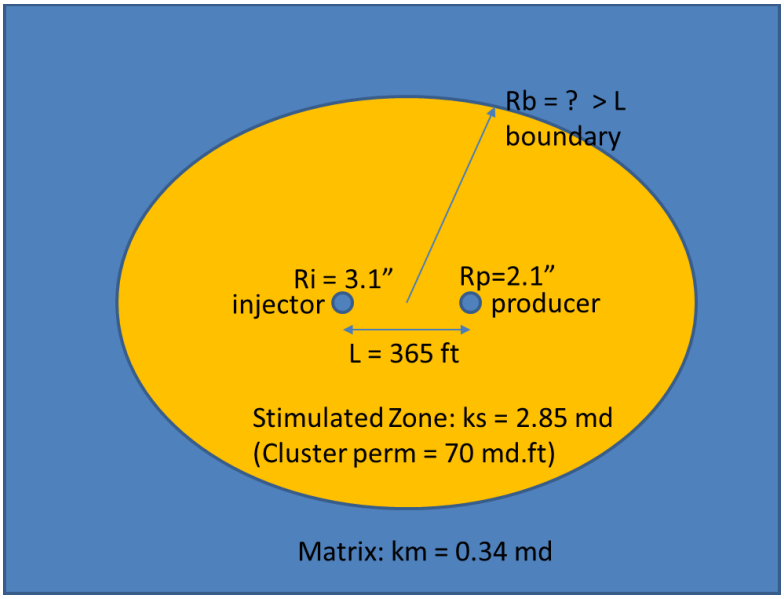

Figure 2: Barrel view of the reservoir model used to estimate the permeabilities of the SRV and the surrounding matrix.

The former time interval (13.5 hrs < t < 42.5 hrs) corresponds to the initial pressurization of the reservoir, with an injection rate of 10 barrels per minute (bpm) while the production well is shut in. As seen in Figure 3, the difference in wellhead pressures (WHP) between the injector and producer remain essentially constant at 204 psi. During this time, the injection temperature is 20 °C, the formation temperature is 185 °C, and the producer wellbore is assumed to be at the static geothermal gradient between these two values. After accounting for hydraulic losses along the injector tubing (estimated at 41 psi using the known tubular geometry and the Colebrook equation) and the thermosiphon pressure associated with the different temperature profiles in the injector and producer (estimated at 190 psi), the inferred difference in bottomhole pressures (BHP) is about 352 psi. Given the two-dimensional radial flow geometry, the permeability k_s of the SRV can be estimated from the formula:

$$P_i(t) - P_p(t) = \frac{Q\eta_{hot}}{2\pi k_s} \ln\left(\frac{L}{R_i}\right) = 352 \text{ psi}, \tag{1}$$

where $Q = 4.1 \times 10^{-5}$ m^2/s is the volumetric injection rate per unit lateral length (after accounting for the expansion of the fluid as a consequence of heating to formation temperature), $R_i = 3.1"$ is the radius of the injection well liner, and η_{hot} is the viscosity of water at 185 °C. Inverting for the permeability yields an average SRV permeability of $k_s = 2.85$ md.

It is also observed in Figure 3 that the pressure transient at the injector (and producer) admits a Theis solution associated with a constant injection rate into a matrix with permeability k_m:

$$P_i(t) - P_i(t_0) = \frac{Q\eta_{hot}}{4\pi k_m} E_1\left(\frac{t_r}{(t-t_0)}\right), \; E_1(y) \equiv \int_y^\infty dy' e^{-y'}. \tag{2}$$

The prefactor of the fit, $\frac{Q\eta_{hot}}{4\pi k_m} = 200$ psi, implies a matrix permeability of $k_m = 0.34$ md beyond the SRV. The relaxation time t_r= 2.4 hrs is related to the pressure (Biot) diffusivity of the fluid and the size of the SRV. Unfortunately, there is not enough information ot infer these two parameters separately.

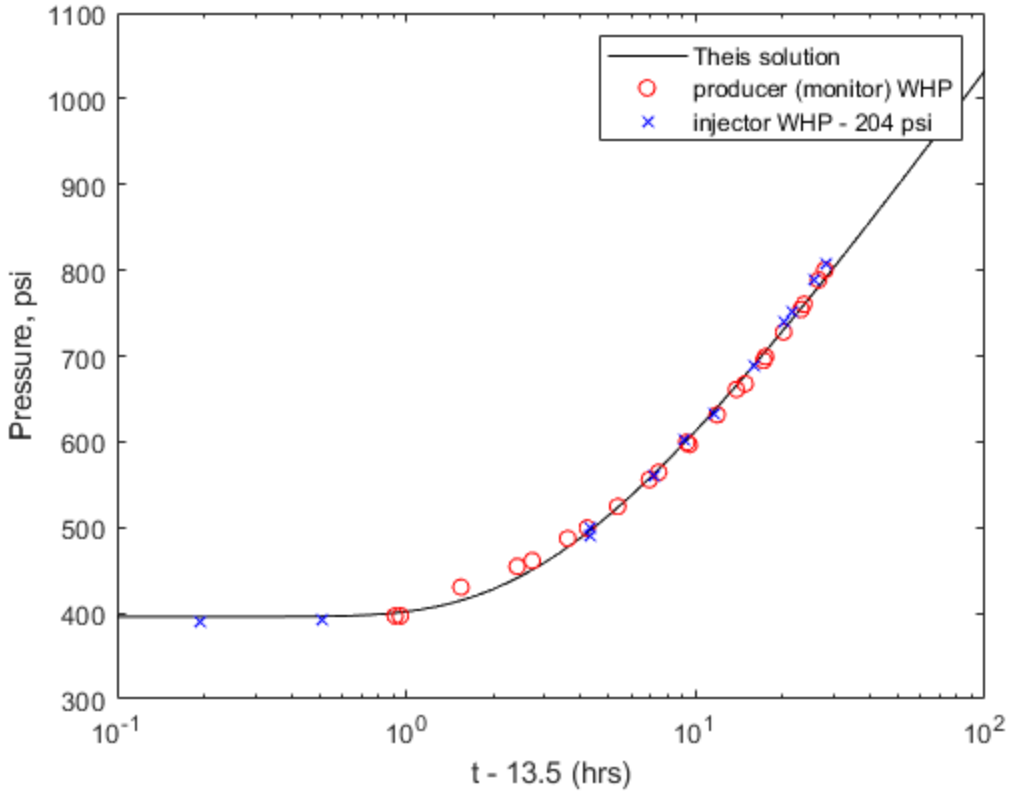

Figure 3: Numerical fit of the pressure transient to the Theis solution. WHP: Well Head Pressure.

The latter time interval (650 hrs < t < 750 hrs) exhibits steady-state flow from injector to producer with a 17.5% leakoff (injection volumetric rate ~ 640 gpm which expands to Q_i ~ 700 gpm downhole, production volumetric rate Q_p ~ 580 gpm). After accounting for hydraulic losses along the injector and producer tubing, as well as the thermosiphon pressure, the interwell BHP drop during this interval is estimated to be about 1120 psi. Substituting into the formula

$$P_i(t) - P_p(t) = \frac{Q_i \eta_{hot}}{2\pi k_s} \ln\left(\frac{L}{R_i}\right) + \frac{Q_p \eta_{hot}}{2\pi k_s} \ln\left(\frac{L}{R_p}\right) = 1120 \text{ psi}, \tag{3}$$

the permeability of the SRV is independently estimated to be $k_s = 2.55$ md, very close to the value inferred from the transient analysis earlier. The corresponding cluster permeability is estimated to be $k_f \sim 60 - 70$ md. ft, somewhat lower than the value inferred by Norbeck and Latimer (2023). Based on private correspondence with the lead author, the discrepancy can be attributed to the following: (i) the equation that was used to infer permeability is not applicable to the prevailing boundary conditions, (ii) thermosiphon pressures were not accounted for, and (iii) leakoff was ignored.

2.2 Thermal Front Propagation and Time to Breakthrough

The reservoir model that was used to fit Project Red circulation test data is simple, but it can be used to predict future performance of the doublet. Of particular importance is the prediction of the movement of the thermal front from the injector towards the producer, and time to thermal breaktrough. To estimate this, consider the general problem of a doublet with well spacing L, N stimulation stages, n clusters/stage and cluster spacing d. For a given **mass** injection rate $\dot{M}$ and production rate $\dot{M}(1-l)$, where l is the leakoff ratio, the Darcy velocity of the fluid along the centerline is given by

$$v(x) = v^*\left(\frac{L}{x} + \frac{(1-l)L}{L-x}\right), \; v^* \equiv \frac{\dot{M}}{2\pi d n N L \rho_{water,hot}}. \tag{4}$$

The thermal front is expected to remain sharp (see Appendix A for a more detailed analysis of the diffuse front), and to propagate at a velocity

$$v_f(x) = \frac{(\rho c_P)_{water,hot}}{(\rho c_P)_{rock}} v(x), \tag{5}$$

where ρc_P is the volumetric heat capacity. The time to thermal breakthrough is given by:

$$t_{BT} = \int_0^L \frac{dx}{v_f(x)} = \frac{(\rho c_P)_{rock}}{(\rho c_P)_{water,hot}} \frac{L}{v^*} \beta, \; \beta \equiv \frac{1}{l^2}\left(\frac{2-l}{2} + \frac{1-l}{l}\ln(1-l)\right). \tag{6}$$

For a given flow rate, the breakthrough time scales with the square of the well spacing.

An immediate conclusion of this analysis is that if Project Red were to be operated at the 640 gpm injection / 580 gpm production rates going forward, based on this simple model it is expected to reach thermal breakthrough in about 5 years provided that flow through the fracture network remains uniform.

3. RESERVOIR OPTIMIZATION

For commercial operation, the goal is to maximize volumetric flow rate per lateral length $q \equiv \frac{Q}{dnN\rho_{water,hot}} = 2\pi v^* L$, subject to a minimum breakthrough time $t_{BT,min}$ dictated by project lifetime, and a maximum interwell pressure drop $P_{h,max}$ dictated by the allowable pressure rise in the formation to alleviate leakoff and potential induced seismicity. The latter is given by:

$$P_h = \int_{R_i}^{L-R_p} \frac{\eta v(x)}{k_s} dx = \frac{\eta v^*}{k_s} \int_{R_i}^{L-R_p} \left(\frac{L}{x} + \frac{(1-l)L}{L-x}\right) dx \tag{7}$$

$$\approx \frac{\eta v^* L}{k_s} \gamma, \qquad \gamma \equiv \ln\left(\frac{L}{R_i}\right) + (1-l)\ln\left(\frac{L}{R_p}\right).$$

Assuming these are the active constraints in the problem, we can simultaneously solve for the optimal well spacing L_{opt} as well as the maximum flow rate q_{max}:

$$q_{max} = \frac{(\rho c_P)_{rock}}{(\rho c_P)_{water,hot}} \frac{2\pi\beta L_{opt}^2}{t_{BT,min}}, \tag{8}$$

$$P_{h,max} = \frac{\eta\gamma}{2\pi k_s} q_{max} \tag{9}$$

For simplicity, we'll assume that γ is held approximately constant, which is consistent with a weakly varying optimal borehole flow velocity when sizing the borehole. With this simplification, we can solve for the optimal values:

$$L_{opt} = \sqrt{\frac{k_s t_{BT,min} P_{h,max}}{\eta\gamma\beta} \frac{(\rho c_P)_{water,hot}}{(\rho c_P)_{rock}}},\ q_{max} = \frac{2\pi k_s}{\eta\gamma} P_{h,max}. \tag{10}$$

As a numerical example, consider a commercial well pad development in an area with 20 °C surface temperature and a geothermal gradient of 50 C/km. The target production is 100 l/s at 200 °C from each injector/producer pair, with an estimated leak-off of 10% at a maximum allowable interwell presure drop of 1000 psi. Assuming an SRV permeability of 2.8 md (similar to Project Red) can be achieved, and targeting a thermal breakthrough time of 30 years, the optimal well spacing is found to be 278 m; somewhat larger than the well separation at Project Red. Whether an equivalent level of stimulation can be achieved at such distances remains an open question.

Consistent with this finding, Fervo Energy has indicated that the well spacing in their Cape Station project will be larger than Project Red. Since only production rates and temperatures from the circulation test were reported in Norbeck et al. (2024), there is not sufficient information available to make an independent assessment of the hydraulic performance of the well and to estimate time to thermal breakthrough.

4. MODEL LIMITATIONS AND CONCLUSION

The hydraulic model presented here has several simplifying assumptions and neglects several important effects, to maintain analytical tractability. It is only intended to make an initial assessment based on short-term injectivity and circulation tests. Variation of SRV permeability as a function of distance from the well for each cluster, as well as cluster-to-cluster and stage-to-stage variations can be incorporated into numerical reservoir models, but the corresponding explosion of the number of fitting parameters is likely to require heavy regularization to yield stable estimates and may not improve the fit to available data. Other consequential physics that has been left out include buoyancy and thermomechanical coupling, whose impact should be studied.

This simple exercise shows the value of measuring and reporting well injectivity and circulation data to build confidence in the commercial viability of the EGS project. Hopefully, the industry will evolve towards a more systematic approach to characterizing EGS reservoirs through standardized injectivity and circulation tests. These measurements are vital to prudent thermal depletion planning.

REFERENCES

Norbeck, J., Gradl, C., and Latimer, T.: Deployment of Enhanced Geothermal System technology leads to rapid cost reductions and performance improvements, EarthArXiV, (2024), https://doi.org/10.31223/X5VH8C. Used under CC BY Attribution 4.0 International.

Norbeck, J.H., and Latimer, T.M.: Verma, A., and Pruess, K.: Commercial-Scale Demonstration of a First-of-a-Kind Enhanced Geothermal System, EarthArXiV, (2023), https://doi.org/10.31223/X52X0B. Used under CC BY Attribution 4.0 International.

APPENDIX

Consider a set of uniform, parallel fracture clusters with spacing d stacked in the y-direction, with a cluster width $h \ll d$ and permeability k_{frac}/h. Water is flowing in the positive x-direction due to a pressure gradient, at a total volumetric flux of $v = -\left(k_{frac}/\eta d\right)\nabla p$. The Darcy velocity of the water in the fracture is $v_w = dv/h$. The inlet of water on the left is at a temperature T_i and the water is invading a formation at temperature T_f. We'll consider the equations that govern heat transfer between the rock and the flowing water in the fracture to determine the shape of the thermal front. For simplicity, we'll ignore the volumetric expansion and changes in volumetric heat capacity $(\rho c_P)_{water}$, $(\rho c_P)_{rock}$ and take the limit $h/d \to 0$. The rock matrix is assumed impermeable, with a constant thermal conductivity κ_f. We then arrive at the following set of PDEs for the temperature profile within the formation $T(x, y, t)$:

$$\frac{\partial T}{\partial t} = \frac{\kappa_f}{(\rho c_P)_{rock}}\left(\frac{\partial^2 T}{\partial y^2} + \frac{\partial^2 T}{\partial x^2}\right), \qquad 0 < y < \frac{d}{2},\ \text{heat conduction in formation}$$

$$\frac{\partial T}{\partial y} = 0, \qquad y = 0,\ \text{symmetry at the midpoint between fractures}$$

$$\kappa_f \frac{\partial T}{\partial y} = -(\rho c_P)_{water} v_w \frac{h}{2}\frac{\partial T}{\partial x}, \qquad y = \frac{d}{2},\ \text{heat transfer to water on the fracture}$$

$$\lim_{x\to-\infty} T = T_i,\ \lim_{x\to\infty} T = T_f,\ \text{limiting temperatures}$$

Integrating the first equation at position x and time t from $y = 0$ to $d/2$, multiplying by $2/d$ and applying the boundary conditions, we obtain:

$$\frac{\partial T_r}{\partial t} = \frac{2\kappa_f}{(\rho c_P)_{rock} d}\left(\left.\frac{\partial T}{\partial y}\right|_{y=d/2} - \left.\frac{\partial T}{\partial y}\right|_{y=0} + \frac{d}{2}\frac{\partial^2 T_r}{\partial x^2}\right) = -\frac{(\rho c_P)_{water} v_w}{(\rho c_P)_{rock}}\frac{h}{d}\frac{\partial T_w}{\partial x} + \frac{\kappa_f}{(\rho c_P)_{rock}}\frac{\partial^2 T_r}{\partial x^2},$$

where $T_r(x,t)$ is the width-averaged temperature of the formation and $T_w(x,t)$ is the temperature of the water in the fracture. Now we rescale units as follows: $\tilde{t} = t/\tau$ where $\tau \equiv (\rho c_P)_{rock} d^2/4\kappa_f$ is the characteristic heat diffusion time, $\tilde{x} \equiv x/(v_f\tau)$ where $v_f \equiv (\rho c_P)_{water} v_w h/(\rho c_P)_{rock} d$ is the characteristic front velocity, and $\tilde{T} = (T - T_i)/(T_f - T_i)$. The equation becomes:

$$\frac{\partial \tilde{T}_r}{\partial \tilde{t}} = -\frac{\partial \tilde{T}_w}{\partial \tilde{x}} + \frac{1}{Pe^2}\frac{\partial^2 \tilde{T}_r}{\partial \tilde{x}^2},$$

$$\lim_{\tilde{x}\to-\infty} \tilde{T} = 0, \lim_{\tilde{x}\to\infty} \tilde{T} = 1.$$

Where the Peclet number $Pe \equiv 2v_f\tau/d = (\rho c_P)_{water} v_w h/\kappa_f$. We now transform to a comoving frame $s = \tilde{x} - \tilde{t}$:

$$\frac{\partial \tilde{T}_r}{\partial \tilde{t}} - \frac{\partial \tilde{T}_r}{\partial s} = -\frac{\partial \tilde{T}_w}{\partial s} + \frac{1}{Pe^2}\frac{\partial^2 \tilde{T}_r}{\partial s^2}$$

Letting $\Delta T = \tilde{T}_r - \tilde{T}_w$, we get a diffusion equation with a source term associated with the temperature differential:

$$\frac{\partial \tilde{T}_r}{\partial \tilde{t}} = \frac{1}{Pe^2}\frac{\partial^2 \tilde{T}_r}{\partial s^2} + \frac{\partial \Delta T}{\partial s}$$

If we neglect the source term, we find that the front spreads over time as an error function:

$$\tilde{T}_r = \frac{Pe}{2}\sqrt{\frac{1}{\pi\tilde{t}}}\int_{-\infty}^{s} ds\, e^{-(Pe\, s)^2/4\tilde{t}}.$$

The characteristic width of the front is given in actual units as

$$w_f(t) = d\sqrt{t/\tau}, t \gg \tau$$

The source term changes the shape of the thermal front, but not its characteristic width. The width of ΔT must match that of $\tilde{T}_r$, therefore $\partial\Delta T/\partial s$ decreases over time as $\sqrt{\tau/t}$ and introduces skewness to $\tilde{T}_r$. The head of the front ends up sharper than the tail. The front develops when $v_f t \gg w_f$, or $t \gg \tau/Pe^2$.

The analysis above is for a planar front. What happens in our 2-D geometry? Even if we ignore the curvature of the front for simplicity, the local front velocity will evolve over time. At early times when the thermal front is closer to the injector,

$$v_f(x) \approx \frac{(\rho c_P)_{water}}{(\rho c_P)_{rock}} v^* \frac{L}{x}, \qquad x \ll L$$

$$t = \int_0^{x_f} \frac{dx}{v_f(x)} = \frac{(\rho c_P)_{rock} x_f^2}{2(\rho c_P)_{water} v^* L}.$$

The ratio of the distance travelled by the front to its width approaches a constant:

$$\left(\frac{x_f}{w_f}\right)^2 \approx \frac{(\rho c_P)_{water}}{2\kappa_f} v^* L \approx \frac{L^2}{t_{BT}\alpha}$$

The thermal front remains relatively sharp provided that the thermal breakthrough time is much shorter than the interwell diffusive relaxation time, which should be true for convection-dominated systems. As an example, for Project Red t_{BT} is about 5 years whereas L^2/α is about 80 years. Therefore, the front width should be about one quarter of the distance traveled by the front. At the midpoint, this gives a front width of about 14 meters, sharper than the planar estimate.